URSI AP-RASC 2019, New Delhi, India; 09 - 15 March 2019

Beam-wave Interaction Analysis of X-band Gridless Reltron

Prabhakar Tripathi[(1)], Arjun Kumar[(1)], Soumojit Shee[(1)], Smrity Dwivedi[(1)] and P.K.Jain[(1)(2)]
(1) IIT–BHU Varanasi, Uttar Pradesh–221005, India, http://www.iitbhu.ac.in
(2) NIT Patna, Patna Bihar–800005, India.

Abstract

In this work, particle in cell (PIC) simulation study has been performed to observe the operating characteristics of the highly efficient gridless-reltron in X-band. A 3D PIC code of gridless reltron is designed using CST microwave studio. The RF interaction structure of the Gridless-reltron is a well-known linac structure *i.e.* side-coupled cavity (SCC). In the reltron, three modes are excited named as 0–mode, $\pi/2$–mode and π–mode. The $\pi/2$–mode is selected as the operating mode because it is unstable and it grows in amplitude. PIC simulation predicts that the modeled gridless reltron with the beam current of 200 A and a total 250 kV as a tube voltage produces a microwave power of ~13 MW at 8.56 GHz with a pulse width of 3.2 μsec and efficiency of ~26%, in the presence of a relatively low guiding magnetic field of 0.40 T.

1 Introduction

Over the last few decades, the research activity on high power microwave (HPM) generation has been drastically increased due to its numerous potential applications, such as in high power microwave radar, as an HPM weapon, HPM testing, and medical application etc. [1]. In present, there are various HPM source generates a microwave power more than of 1GW, like a relativistic backward wave oscillator (RBWO), vircator, the magnetically insulated line oscillator (MILO), relativistic klystron oscillator (RKO), transit time oscillator (TTO) and super reltron. Such huge microwave power generation is possible due to the use of explosive emissive cathode which generates an intense relativistic electron beam (IREB). The explosive emissive cathode inherently suffered from a problem called plasma formation which is the prime factor of pulse shortening. This plasma formation in the HPM source limits its long pulsed operation [2-4].

Super reltron is a newest slow wave microwave oscillator and mainly divided into two categories first one is gridded reltron, and the second one is gridless reltron. Gridded reltron uses a velvet cathode to generate an electron beam which is an example of explosive emission cathode. The gridded reltron generate more than 600 MW output power in L–band and 400 MW in the S–band with a pulse width

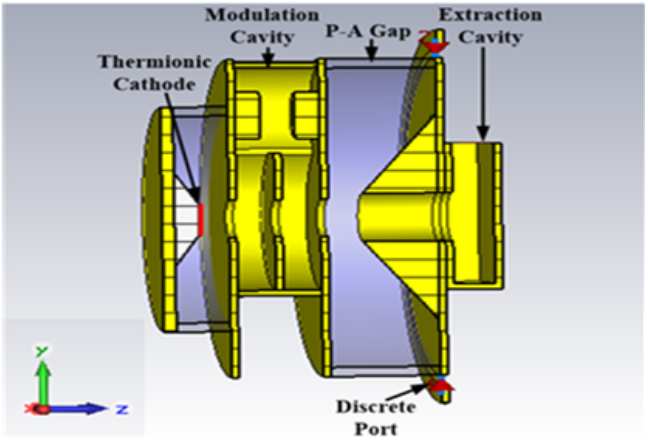

Figure 1. 3D Schematic diagram of gridless reltron.

of a few hundreds of nsec [4]. The prime advantage of the gridded reltron is, it does not require any external magnetic field for guiding electron beam while the main constraints of gridded reltron are that it is suffered from pulse shortening and having low PRR. The second variant of super reltron is gridless reltron which uses thermionic cathode for the electron beam generation, and it requires a low external magnetic field for guiding the electron beam. Since it uses a thermionic cathode, the chance of plasma formation is less as compared to the gridded reltron thus a long pulse operation can be achieved. Miller *et al.* [5] reported an experimental gridless reltron in S-band reported and obtained 20 MW power, 5μsec pulse width, and 100 Hz PRR [5].

In this paper, highly efficient gridless reltron in X-band is designed using CST Microwave studio[8] and investigate its RF behavior and PIC performance. In section II, a working mechanism of the device, its subsection, and a typical design parameter is discussed. In section III, 1D single particle analysis has been performed and obtained simulation results is discussed in section IV. Finally, in Section V, a summary and conclusion are given.

2 Working Principle

A 3D schematic diagram of a gridless reltron is shown in figure 1. The gridless reltron comprised of the thermionic cathode, RF interaction structure, and extraction cavity. The thermionic cathode is used to generate an electron

beam. The RF interaction structure *i.e.* modulation cavity converts the continuous electron beam into bunches. A high DC pulse voltage is applied just after the RF interaction structure *i.e.* in the post-acceleration gap. This post-acceleration DC pulse accelerates the electron bunches at a relativistic velocity which exit from the RF interaction structure. The relativistic velocity increases the kinetic energy of the electron beam and reduces the relative kinetic energy spread of electrons. Multiple extraction cavities are used for the extraction of microwave power from the electron beam bunches. Finally, a beam dump is used to collect the unused electron beam [2].

The RF interaction structure of the gridless-reltron is a well-known linac structure *i.e.* side-coupled cavity (SCC), which is comprised of the one metal disc, and two cavities named as coupled cavity and the main cavity. The coupled cavity is placed radially at the top of the main cavity and metal disc is placed at the center of the main cavity which divides the main cavity into two equal parts named as front and rear main cavity. This three cavity system has three resonant modes, 0–mode, $\pi/2$–mode and π–mode. In 0–mode, the electric field in the main cavity and coupled cavity are in phase while in π–mode the electric field in the main cavity and coupled cavity are out in phase. However in $\pi/2$–mode electric field in a coupled cavity is zero and electric field in front and rear main cavity is out of phase. Out of these three modes we select $\pi/2$–mode as an operational mode, because $\pi/2$–mode is only unstable mode. The design parameter is calculated from the Miller *et al.* [2] and summarized in table 1.

Table 1. Design Parameter of Gridless Reltron

Parameter	Dimension(mm)
Main Cavity Radius	12.76
Coupled Cavity Radius	6.38
Idler Radius	3.19
Hole Radius	4.0
Spacing Between Metal Disc	5.71
A-K Gap	6.28
Drift Tube Length	12.74
Post–Acceleration Gap	16.98

3 1D Single Particle Analysis

1D single particle analysis has been performed to show, that the RF interaction structure will self-excite. The whole longitudinal space of the RF interaction structure is divided into multiple equal spatial cells of length δz . Using the concept of courant stability condition (*i.e.* $\delta t \leq \delta z/c$)) the time period of the spatial cell is determined. An electron launch into the RF interaction structure at a specific phase angle φ and track its velocity and displacement as it transits the 1^{st} and 2^{nd} gap of the cavity. The electron's kinetic energy is calculated from its velocity at the end of the 2^{nd} gap [6,7].

It is assumed that the amplitude of the saturated electric field is constant and the polarity of the electric field is varied by 180^0 in the front and rear main cavity. The equation of the electric field in the front and rear main cavity is expressed as.

$$E_z(t) = +E_{z0}\cos(\omega t + \varphi) \qquad for\ 0 \leq z \leq g \tag{1}$$

$$E_z(t) = -E_{z0}\cos(\omega t + \varphi) \qquad for\ g \leq z \leq 2g \tag{2}$$

The equation of velocity and displacement in the 1st cavity and in the 2^{nd} cavity is given by [6,7].

$$v_1(t,\varphi) = v_0 + \frac{qE_{z0}}{m_e\omega}(\cos(\omega t + \varphi) - \cos(\varphi)) \tag{3}$$

$$z_1(t,\varphi) = v_0 t + \frac{qE_{z0}}{m_e\omega^2}(\sin(\omega t + \varphi) - \sin(\varphi) - \omega t\cos(\varphi)) \tag{4}$$

$$v_2(t,\varphi) = v_1 - \frac{qE_{z0}}{m_e\omega}(\cos(\omega t + \varphi) - \cos(\varphi)) \tag{5}$$

$$z_2(t,\varphi) = v_1 t - \frac{qE_{z0}}{m_e\omega^2}(\sin(\omega t + \varphi) - \sin(\varphi) - \omega t\cos(\varphi)) \tag{6}$$

where c, ω, φ, g, v_1, z_1 and v_2, z_2, are the speed of light, resonating frequency, phase space, spacing between the front and rear main cavity, velocity and displacement in the 1^{st} gap and 2^{nd} gap respectively while v_1 is the velocity of an electron at a time when it enters into the 2^{nd} gap. Figure 2, shows the velocity of an electron at the phase angle of $\varphi = 0.52\pi$. From figure 2, it is clearly seen that electron is deaccelerating in the 1^{st} gap and accelerating in the 2^{nd} gap of the RF interaction structure. The electron enters the 1^{st} gap with an initial velocity of 0.54822c and exits from the 2^{nd} gap with velocity 0.5368c. The exit velocity of the electron is less than the initially entered velocity of the electron This change in the velocity (*i.e.* kinetic energy) of an electron results gains in electromagnetic energy inside the cavity.

This analysis is repeated for the whole phase period i.e. from 0 to 2π. Figure 3, shows the plots of the normalized kinetic energy of electrons for different phase angles. From figure 3, it is clearly observed that the electrons are gaining kinetic energy for the phase angle $0 \leq \varphi \leq 0.2\pi$ to $1.08\pi \leq \varphi \leq 1.26\pi$ and for the rest phase angle electron loses its kinetic energy in the cavity. Since electrons lose energy for large phase angle as a comparison with the electrons gains energy for a very small phase angle. This imbalance of the energy exchange in the cavity shows that the cavity is self-excited.

4 Simulation Results

For a better understanding of device and its working mechanism, the device is designed using the 3D PIC code CST Particle studio as shown in figure 1. The dimensional parameters of the Gridless-reltron in X-band shown in table 1 are derived using the literature reported by Miller *et al.* [2].

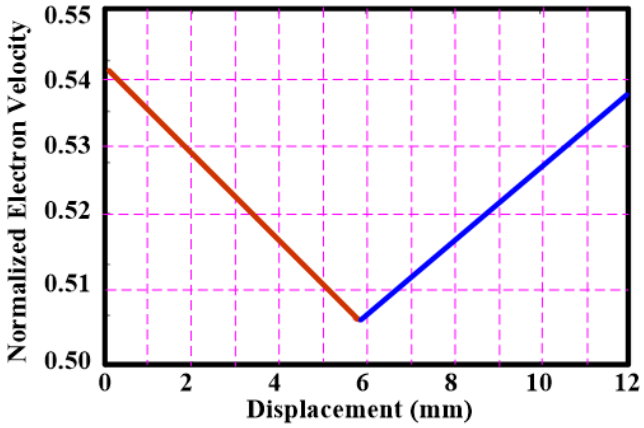

Figure 2. Electron velocity for $\varphi = 0.52\pi$.

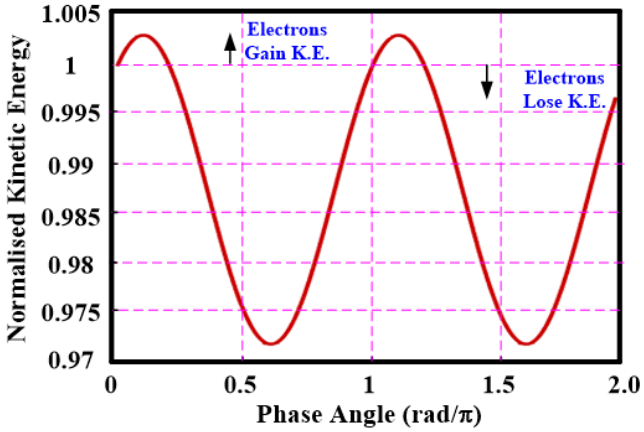

Figure 3. The kinetic energy of output electron as a function of phase angle.

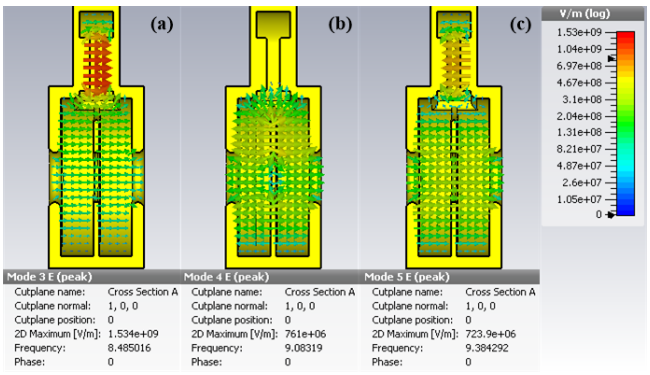

Figure 4. Electric field pattern generated in the modulation cavity..

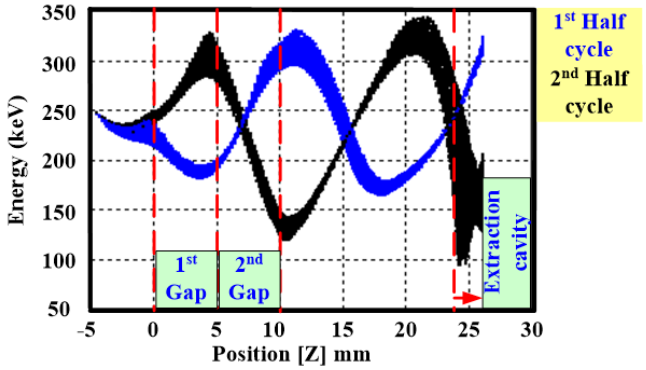

Figure 5. The plot of the electron's phase space.

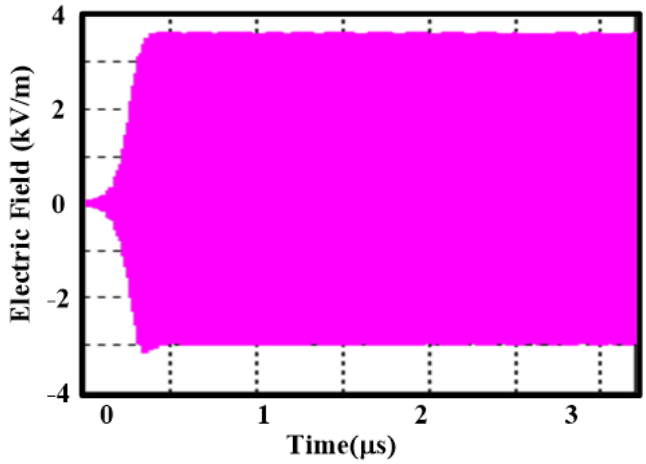

Figure 6. Electric field developed inside the extraction cavity.

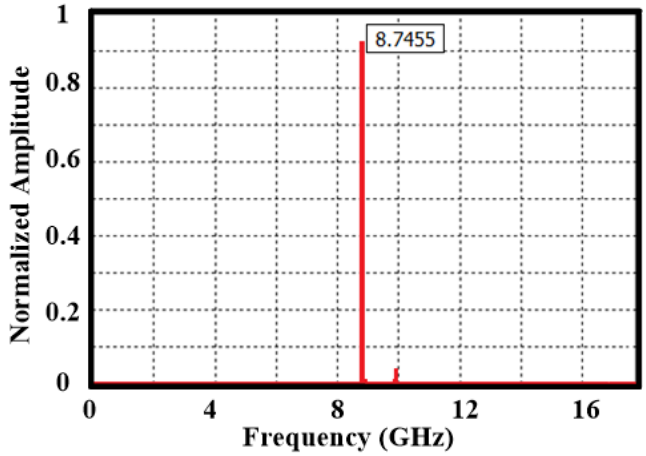

Figure 7. The frequency spectrum of the electric field intensity

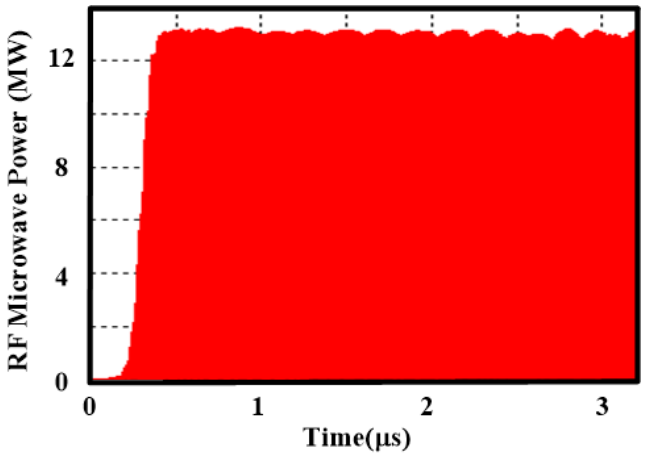

Figure 8. Microwave power developed at the output port.

4.1 Eigenmode Solver

The electromagnetic behavior of the modulating cavity is analyzed by using CST Eigenmode solver. The obtained results from the Eigenmode solver are shown in figure 4. The figure 4 (a), 4 (b) and 4 (c) show that 0–mode, $\pi/2$–mode and π–mode resonates at 8.47 GHz, 9.08 GHz, and 9.376 GHz respectively.

4.2 PIC Simulations

A 3D PIC CST code is used to observe the RF behavior of the device. Before starting a simulation, we select a space phase monitor function which records the kinetic energy of electron with respect to their position. Waveguide port is applied at the extractor cavity which records the generated electric field inside the extraction cavity with respect to the time. For electron source a thermionic emission model is selected with 1 nsec rise time, beam current of 200 A, and the kinetic energy of 100 keV. A discrete port function is used to provide the post-acceleration voltage. A DC step signal of 3200 nsec duration with a rise time of 1 nsec as an excitation signal is applied to the discrete port. We used the total tube voltage of 250 kV in which 100 kV voltages are applied to the thermionic cathode and rest voltage i.e. 150 kV is applied to the post-acceleration gap. Figure 5, shows the kinetic energy distribution of the electrons in gridless reltron. From figure 5, it can be clearly observed that during the 1^{st} half RF cycle the electrons get deaccelerated in the 1^{st} gap and then accelerated in the 2^{nd} gap when it traverses the gap. During the 2^{nd} half RF cycle, the electrons encounter a reverse Lorenz force and get accelerated in the 1^{st} gap and deaccelerated in the 2^{nd} gap of the modulating cavity. The acceleration and deceleration of the electrons cause a velocity modulation and a lead to the formation of electron bunches. When these electrons bunch reached to the extraction cavity, they give their kinetic energy to the electromagnetic field which is present in the extraction cavity. The amplitude of the electric field intensity which is developed in the extraction cavity, shown in figure 6. The operating frequency is calculated by taking a Fast Fourier Transform (FFT) of the electric field intensity developed in the extraction cavity. In Figure 7, the operating frequency of 8.7455 GHz which is 33.45 MHz lower than the resonating frequency predicted by Eigenmode solver. This frequency shift is occurred due to the beam loading effect. The microwave power developed at the extraction cavity is in dominant TE_{10} mode. From figure 8, it is observed that the RF microwave power generated at the output port is 13 MW.

5 Conclusion

In this work, we have successfully simulated the gridless reltron in X-band with the help of the 3D PIC CST code. The optimized 3D PIC CST code of X-band gridless reltron generates microwave power of ~13 MW at frequency of 8.7455 GHz with a pulse width of 3.2 μsec and an efficiency of ~26%, when supplied with the total tube voltage of 250 kV, beam current of 200 A, and a relatively low guiding magnetic field of 0.40 T.

References

[1] James Benford, John A. Swegle, and Edl Schamiloglu, "High power microwaves," CRC Press, 2007, ISBN 9781482260595.

[2] R. B. Miller, W. F. McCullough, K. T. Lancaster, and C. A.Muehlenweg, "Super-reltron theory and experiments," IEEE Trans. Plasma Sci., vol. 20, no. 3, pp. 332âĂŞ343, Jun. 1992, doi:10.1109/27.142834

[3] R. B. Miller, W. F. McCullough, K. T. Lancaster, and C. A. Muehlenweg, "Super-reltron analysis and experiments,", In Microwave Symposium Digest, Jun. 1992., IEEE MTT-S International, pp. 237-240, doi:10.1109/MWSYM.1992.187955

[4] R. B. Miller, C. A. Muehlenweg, K. W. Habiger, and J. R. Clifford, "Super-reltron progress," IEEE Trans. Plasma Sci., vol. 22, no. 5, pp. 701âĂŞ705, Oct. 1994. doi:10.1109/27.338285

[5] R. B. Miller, K. W. Habiger, W. R. Beggs, and J. R. Clifford, "Advances in super-reltron source development," In Intense Microwave Pulses III, vol. 2557, pp. 2-9, International Society for Optics and Photonics, 1995, doi:10.1117/12.218534

[6] Soh, Shawn. "Modeling, simulation and experimental study of the UNM low power reltron," (2012). https://digitalrepository.unm.edu/ece_etds/240

[7] S. Soh, E. Schamiloglu, and R. B. Miller, "Dual cavity reltron, In Pulsed Power Conference (PPC), pp. 653-657, IEEE, 2011, doi:10.1109/PPC.2011.6191557

[8] User's Manual, CST-Particle Studio, Darmstadt, Germany, 2014.